

Article

The Kinetic Aspects of the Dissolution of Slightly Soluble Lanthanoid Carbonates

Tatiana Litvinova, Ruslan Kashurin *, Ivan Zhadovskiy  and Stepan Gerasev

The Department of Physical Chemistry, Saint-Petersburg Mining University, 199106 St. Petersburg, Russia; litvinova_te@pers.spmi.ru (T.L.); Zhadovskiy_IT@pers.spmi.ru (I.Z.); s212382@stud.spmi.ru (S.G.)

* Correspondence: s195002@stud.spmi.ru

Abstract: The problem of the complex use of mineral raw materials is significant in the context of many industries. In the rare earth industry, in the context of limited traditional domestic reserves and dependence on imports of lanthanides, an unambiguous and comprehensive solution has not yet been developed. Promising areas include the involvement of technogenic raw materials in the industrial turnover. The present study examines the kinetics of the dissolution process of poorly soluble lanthanide compounds when changing the parameters of the system. The results obtained reflect the dependence of the degree of extraction of lanthanide on the following variable parameters of the system: temperature, concentration of the complexing agent, and intensity of mixing. On the basis of the experiment, the values of the activation energy and the reaction orders were calculated. The activation energy of the carbonate dissolution process, in kJ/mol, was as follows: 61.6 for cerium, 39.9 for neodymium, 45.4 for ytterbium. The apparent reaction orders of the carbonates are equal to one. The prospect of using the research results lies in the potential to create a mathematical model of the process of extracting a rare earth metal by the carbonate alkaline method.



Citation: Litvinova, T.; Kashurin, R.; Zhadovskiy, I.; Gerasev, S. The Kinetic Aspects of the Dissolution of Slightly Soluble Lanthanoid Carbonates. *Metals* **2021**, *11*, 1793. <https://doi.org/10.3390/met11111793>

Academic Editors: Carlos Capdevila-Montes and Antonije Onjia

Received: 20 September 2021

Accepted: 5 November 2021

Published: 8 November 2021

Publisher's Note: MDPI stays neutral with regard to jurisdictional claims in published maps and institutional affiliations.



Copyright: © 2021 by the authors. Licensee MDPI, Basel, Switzerland. This article is an open access article distributed under the terms and conditions of the Creative Commons Attribution (CC BY) license (<https://creativecommons.org/licenses/by/4.0/>).

Keywords: carbonate; isotherm; dissolution; rare earth metals; technogenic raw materials; lanthanides; mud

1. Introduction

The need for the integrated processing of raw materials entails the principles of environmental law, in terms of both the rational use of resources and the protection of life and health. The increase in the world population, as well as its consumer abilities, is accompanied by an increase in production capacity. The high degree of automation and the development of new technologies requires an increasing number of economic and mineral resources, which, in turn, pollute the environment. The annual increase in the volume of human-made waste contributes to an increase in the cost of environmental measures for the disposal of sludge, their storage, and transportation.

Rare earth metals are essential raw materials for developing industries. However, methods of producing REM from traditional sources require considerable investment. The raw materials for producing REM can be minerals such as loparite, monacite, gadolinite, and pegmatite, etc. Currently, the direction of obtaining rare earth metals from technogenic raw materials is actively developing, including red mud, phosphogypsum, coal, and ash slag waste.

According to literary data, a significant amount of La, Ce, Pr, Nd, and other rare earth elements, with a sum of REM from 0.5 to 2.5 kg/t [1], including from 90 to 110 g/t Sc₂O₃ [2], are found in red mud. The data in Ref. [3] indicate the content of scandium, yttrium, lanthanum, and ytterbium in the feedstock (bauxites). The sum of REM oxides is more than 1 kg/t.

In the production of 1 ton of fertilizers, 1.5–4.5 tons of phosphogypsum occurs as non-poisonous, but unsuitable waste. Rare earth metals may be contained in apatite feedstocks. Due to their conversion to sulphate solutions, rare earth metals gradually pass

into dumps [4–6]. The accumulation of red mud, which increases up to 1.5 tons per 1 ton of ore processed, can cause an environmental disaster [7,8]. The amount of stored red mud wastes is growing every year and may reach up to 200 million tons in the near future. The costs of the largest companies for the production of mineral fertilizers and aluminum for environmental protection enterprises will only grow.

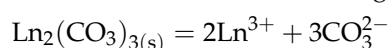
The problem of recycling red mud can be solved in various ways, the process diagram is described in detail by the authors in works [9,10]. Preferably, it is proposed to sinter sludge [11], use the waste in iron smelting, and use the waste as catalysts of the chemical industry, as well as in the construction industry [12–14]. Thus, red muds are wastes that make up a significant share of the costs of production, on the other hand they are valuable raw materials. The following components of red mud are of great value: iron, titanium, and scandium, as well as rare earth elements [15]. However, this type of human-made raw material cannot be used without sufficient dewatering; however, these aspects have already been considered in the works [16,17].

The vast majority of scientific works are devoted to the extraction of REM from human-made raw materials using mineral acids (hydrochloric, nitric, and sulfuric acids). Disadvantages of acid-leaching technologies include the high cost of reagents, insufficient degree of recovery (mainly from 30 to 80%), as well as the economic inexpediency of extraction process from solutions by, for example, nitric acid [18]. In works [19–22], aspects of extraction of rare-earth metals by the method of extraction from various technogenic sources are considered. With regard to the use of both the acidic treatment of red mud and the extraction of REM, it is worth noting that such a method is poorly applicable to highly alkaline red mud. In work [23], the applicability of rare-earth metal sorption is considered. There is also information on less common methods of extraction, for example, using nanomaterials [24]. It is the high alkali content that is one of the factors complicating the processing of this waste.

There are various technologies for processing red mud, in particular, those discussed in scientific study [25]. Currently, there is a technology of processing red mud using carbon dioxide, which allows the extraction of scandium [26,27]. The technology of scandium extraction from red mud using carbon dioxide of exhaust gases was developed [3]. However, scandium is quite different from lanthanides, so it is not possible to stably recover lanthanides by the same industrial method.

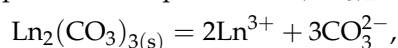
It should be noted that, in the proposed process modes, the degree of recovery of lanthanides is unstable and most REM remain mainly in the composition of the sludge. In order to carry out the complex extraction of REM from sludges, it is necessary to determine the thermodynamic and kinetic parameters of the lanthanide–carbonate–alkali system. Using these data, it becomes possible at various stages of the process to transfer rare earth metals from sludge to solution, separate scandium, and then separate light and heavy lanthanides. The extraction method makes it possible to obtain extraction of rare-earth metals, as shown by a number of works [28,29]. When processing phosphate raw materials, stability of phosphate complexes of lanthanides should be taken into account [30].

Lanthanide ions are very active and form naturally insoluble salts, for example carbonates. Low equilibrium constants, related to the following reaction:



are presented in Table 1.

Apparently, an excess of carbonate ions is needed to dissolve the slightly soluble salt. In parallel with displacement, water-soluble complexes are formed. Carbonate treatment of red mud converts water-insoluble carbonates to stable carbonates, according to Wood and Millero [31], carbonate complexes of composition $\text{Ln}(\text{CO}_3)_2^-$, by the following reaction:



where M is an alkali metal or ammonium cation.

Table 1. Dissolution constants.

| Element | logK |
|---------|--------|
| La | −35.1 |
| Ce | −35.3 |
| Pr | −34.8 |
| Nd | −34.65 |
| Sm | −34.5 |
| Eu | −35.0 |
| Gd | −34.7 |
| Tb | −34.2 |
| Dy | −34.0 |
| Ho | −33.8 |
| Er | −33.6 |
| Tm | −33.4 |
| Yb | −33.3 |
| Lu | −33.0 |

The economy, selectivity, and recoverability of carbonates are the main advantages of carbonate leaching over acid leaching. The potential use of spent carbonate solutions in the chemical and agricultural industries is also important.

For mathematical modeling of the process of extraction of rare-earth metals (REM) from human-made raw materials, the main thermodynamic and kinetic parameters of the process of carbonation of REM deposits should be determined. The process of dissolving slightly soluble compounds does not have a thermodynamic prohibition but seems to be limited by kinetic features.

The aim of the present study is to establish the kinetic parameters of the process of dissolving carbonates, light lanthanide hydroxides (Ce, Nd), and a member of the heavy group, REM–ytterbium (Yb).

2. Materials and Methods

Synthetic preparations of lanthanide carbonates and hydroxides were used to study the kinetic features of complex formation. They are obtained by inorganic synthesis methods, namely, by precipitation from solutions of the corresponding nitrates of chemically pure lanthanides. Reliability of composition of obtained REM preparations is confirmed by analysis of obtained precipitates by methods of X-ray powder diffractometry and X-ray fluorescence analysis, applicability of these methods is specified in [32]. Part of the study is performed in Ref. [33]. Precipitation dissolution is carried out in chemically pure potassium carbonate.

Dissolution of lanthanide carbonates and hydroxides was carried out in static mode at the HEL Auto-MATE Reactor System, which ensures maintenance of process parameters, such as mixing speed, temperature, and the pH of the solution. The sizes of the powder particles were investigated using MicroSizer-201C. The integrated diagram is shown in Figure 1.

The dimensions of the fractions are shown in Table 2.

The conditions of the experimental studies are shown in Table 3.

Analysis of the lanthanide content in the solution was performed on the basis of weight loss during REM preparation suspension, and on the results of the complexometric analysis of solution in presence of arsenazo (III) [34]. The degree of REM recovery into solution was determined by the following equation:

$$E_{Ln} = \frac{C_{Ln} \cdot V_1 \cdot M_{Ln s}}{m_s} \cdot 100\%,$$

where: E_{Ln} —the degree of ion recovery into the solution Ln^{3+} (%); C_{Ln} —molar concentration of lanthanide ions in final solution (mol/L); V_1 —liquid phase volume, l; $M_{Ln s}$ —molar mass of lanthanide precipitate (g/mol); m_s —weight of lanthanide sediment suspension (g).

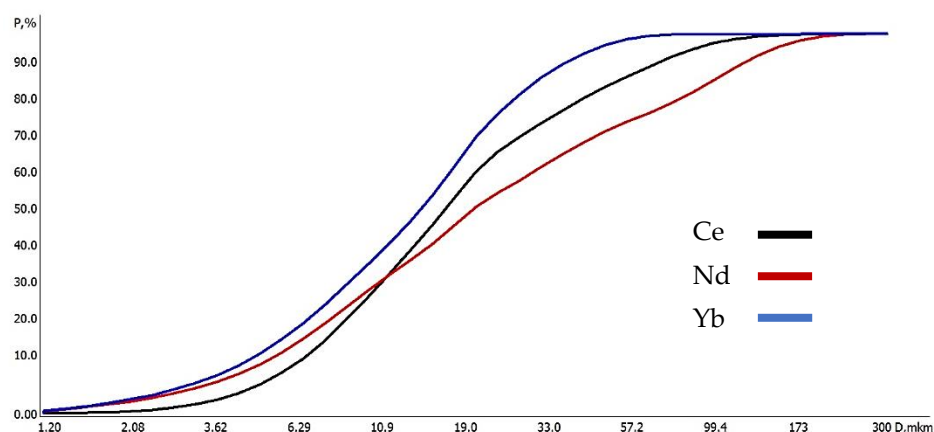


Figure 1. Granulometry of powders.

Table 2. Size of fractions.

| Element | | P, % | | | | | | | |
|------------|------|------|------|------|------|------|------|------|-------|
| Ce | 0.1 | 0.5 | 1.4 | 3.2 | 6.2 | 11.0 | 18.1 | 27.6 | 37.8 |
| Nd | 2.1 | 3.4 | 5.3 | 7.8 | 11.4 | 16.3 | 22.7 | 30.2 | 37.1 |
| Yb | 2.4 | 4.1 | 6.3 | 9.5 | 13.9 | 19.9 | 27.5 | 36.5 | 45.7 |
| D, microns | 2.02 | 2.54 | 3.2 | 4.03 | 5.08 | 6.40 | 8.06 | 10.2 | 12.8 |
| Ce | 48.5 | 59.5 | 69.7 | 75.8 | 81.5 | 86.1 | 89.6 | 95.0 | 97.7 |
| Nd | 43.9 | 51.4 | 58.6 | 64.3 | 69.8 | 74.4 | 77.6 | 83.1 | 88.4 |
| Yb | 56.1 | 68.1 | 79.8 | 87.8 | 93.6 | 97.1 | 99.0 | 99.7 | 99.7 |
| D, microns | 16.1 | 20.0 | 25.6 | 32.3 | 40.6 | 50 | 60 | 81.3 | 102.0 |

Table 3. Parameters of sediment carbonation of REM.

| Process Parameter | Value | Dimension |
|--|-----------|-----------|
| Concentration CO_3^{2-} in solution | 0.5–1.5 | mol/L |
| Agitation intensity | 1000 | rpm |
| Temperature | 293–313 | K |
| Mixing time | 0.5–50 | min |
| pH | 11.5–12.0 | - |
| Ratio l:s | 2100 | mL/g |

3. Results

During the study, experimental relationships were obtained for the recovery of lanthanide into solution. The following absolute concentrations of lanthanides in solution were obtained: 1.2–2.05 mmol/L for Ce; 0.5–1.75 mmol/L for Nd; 0.67–1.58 mmol/L for Yb. The values were then converted to E_{Ln} . The effect of the concentration of potassium carbonate solution on the recovery rate of lanthanides at 20 °C, with the stirring rate of 1000 rpm is shown in Figure 2.

Dependencies with an approximation validity of at least 98% are described by logarithmic dependencies (Table 4), which suggests the first order of the leaching reaction.

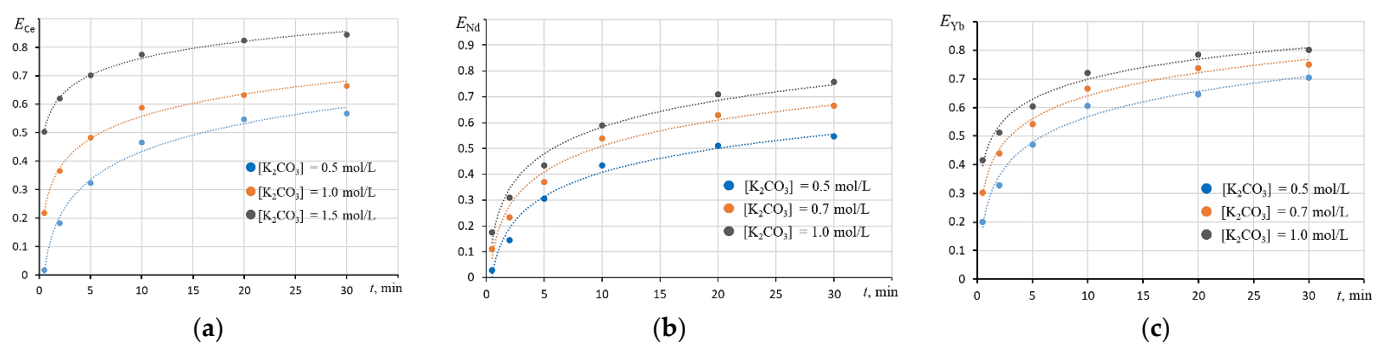


Figure 2. The extent to which lanthanides are recovered depends on the concentration of potassium carbonate: (a) for Ce; (b) for Nd; (c) for Yb.

Table 4. Empirical dependence of the degree of recovery into the solution on the concentration of potassium carbonate.

| $[K_2CO_3]$, mol/L | Dependency Equation (Nd) | Dependency Equation (Yb) |
|---------------------|-----------------------------|-----------------------------|
| 0.5 | $y = 0.1346\ln(x) + 0.0972$ | $y = 0.1282\ln(x) + 0.2724$ |
| 0.7 | $y = 0.1452\ln(x) + 0.1752$ | $y = 0.1161\ln(x) + 0.3738$ |
| 1 | $y = 0.1492\ln(x) + 0.2393$ | $y = 0.1008\ln(x) + 0.4667$ |
| $[K_2CO_3]$, mol/L | Dependency Equation (Ce) | - |
| 0.5 | $y = 0.1424\ln(x) + 0.1059$ | - |
| 1 | $y = 0.1127\ln(x) + 0.2983$ | - |
| 1.5 | $y = 0.0857\ln(x) + 0.5645$ | - |

Due to the fact that the leaching was carried out with an excess of potassium carbonate, the effect of the concentration of the solution on the degree of recovery is mainly due to a shift in equilibrium towards the reaction products, according to the Le Chatelier principle, and it has little effect on the kinetic parameters of the process. A close to equilibrium state was achieved with a stirring time of 10 min, which was characterized by a negligible effect of the phase contact time on the recovery rate. The effect of the stirring rate on the recovery rate of lanthanide carbonate into the solution at 20 °C, and the concentration of potassium carbonate solution of 1 M, is shown in Figure 3.

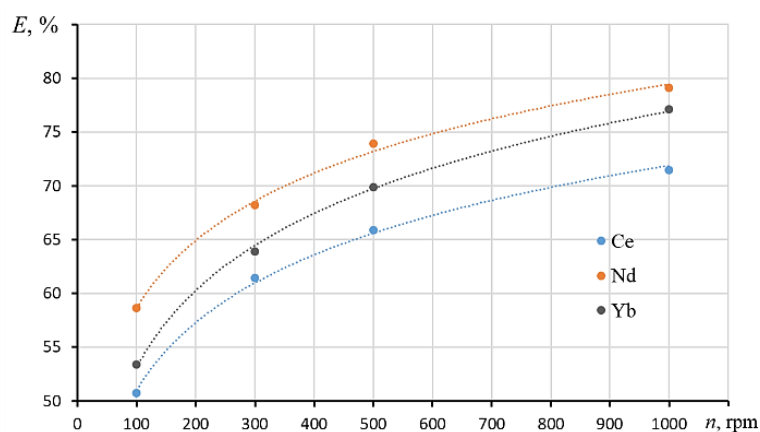


Figure 3. Lanthanide recovery rate versus mixing rate at a phase contact time of 10 min.

The degree of recovery decreases in the direction from neodymium to cerium, which may be due to differences in the activation energy of lanthanide carbonate leaching. An

increase in the mixing rate led to an increase in the degree of recovery into the solution, which is characteristic of processes limited by the external diffusion of reagents. The effect of temperature (in 1 M potassium carbonate solution and 1000 rpm) is shown in Figure 4.

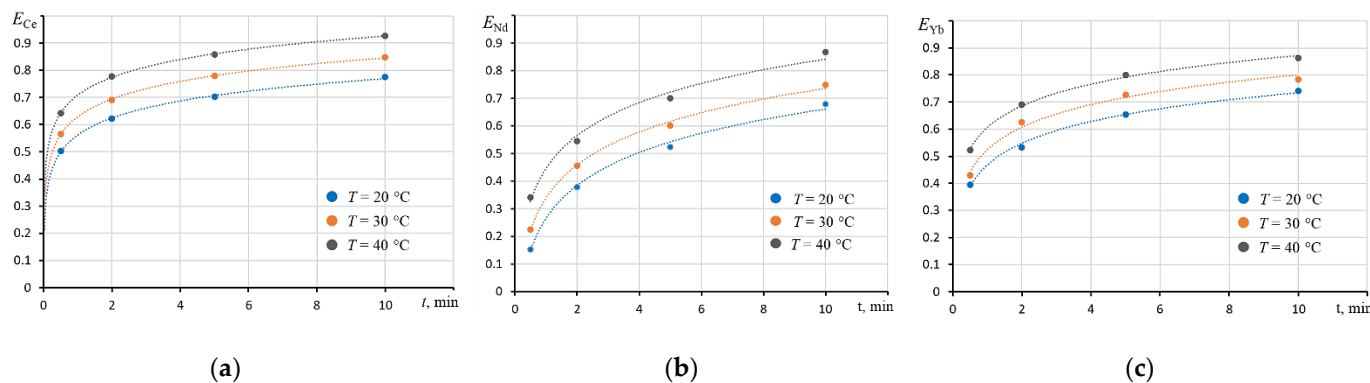


Figure 4. Dependence of lanthanide recovery on temperature and stirring time: (a) for Ce; (b) for Nd; (c) for Yb.

An increase in temperature led to a regular increase in the degree of extraction. The dependencies were approximated by logarithmic dependence with a validity of 98%, the empirical approximation equations are shown in Table 5.

Table 5. Degree of extraction versus time and temperature.

| $T, ^\circ\text{C}$ | Nd | Yb | Ce |
|---------------------|-----------------------------|-----------------------------|-----------------------------|
| 20 | $y = 0.1719\ln(x) + 0.2658$ | $y = 0.1158\ln(x) + 0.4679$ | $y = 0.0898\ln(x) + 0.5625$ |
| 30 | $y = 0.1724\ln(x) + 0.3395$ | $y = 0.1201\ln(x) + 0.5243$ | $y = 0.0938\ln(x) + 0.6295$ |
| 40 | $y = 0.1719\ln(x) + 0.4461$ | $y = 0.1154\ln(x) + 0.6063$ | $y = 0.0944\ln(x) + 0.7087$ |

The logarithmic approximation of the extraction degree, versus time dependencies obtained at different temperatures, indirectly indicated the first order of the reaction.

4. Discussion

The reaction proceeds through a series of successive steps that involve external and internal diffusion of the reagent from the solution to the surface of solid phase, adsorption, reaction on surface solid phase, desorption of product, and reverse mass transfer of product to liquid phase. The solid phase, in the form of a fine powder, is mixed with the liquid solution, while constantly suspended. The particles of the dispersed phase do not have a porous structure, which makes it possible to not take into account the stage of internal diffusion. To describe the patterns of the process, it is first necessary to determine its limiting stage, reaction order and process-activation energy. There are various mathematical models describing a heterogeneous reaction.

We took into account the dependence of the degree of extraction on the concentration of carbonate and the rate of mixing. The effective diffusion layer model was selected. It describes the kinetics of the process. This method is widely used to describe leaching [35–37]. The method allows you to establish the order of the reaction and the effective activation energy. The combination of these parameters allows you to identify the limiting stage of the process.

If the chemical reaction itself proceeds quickly enough, then the concentration of the substance at phase boundary = 0 and the reaction rate equation takes the form of a first-order equation as follows:

$$w = \beta C_0$$

Since potassium carbonate is in excess with respect to rare earth metal carbonate, the process rate and the change in sample weight is determined by the amount of lanthanide

carbonate that entered the complexing reaction, and the kinetic equation is recorded as follows:

$$w = \frac{dm_t}{dt} = \beta m_t$$

where β —mass transfer factor; m_t —weight of lanthanide carbonate.

Accordingly, the dependence of the logarithm of lanthanide carbonate mass against time must be linear, with an angular coefficient corresponding to the mass transfer coefficient. The semilog time-dependent weight of lanthanide carbonate, based on studies of the effect of temperature and potassium carbonate concentration on the degree of lanthanide recovery into solution, is shown in Figures 5 and 6.

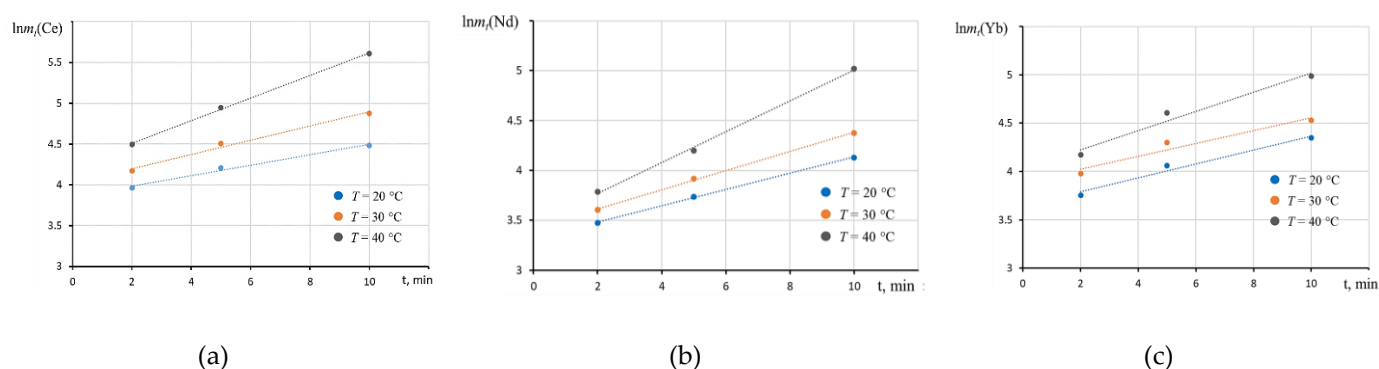


Figure 5. Time-dependent logarithm of weight, obtained by dissolving lanthanide carbonate in 1 M potassium carbonate solution at different temperatures: (a) for Ce; (b) for Nd; (c) for Yb.

The resulting dependencies are satisfactorily approximated by the linear dependencies shown in Table 6. The value of approximation validity was less than 96%.

Table 6. Degree of extraction versus time and temperature in linear form.

| T, °C | Nd | Yb | Ce |
|-------|------------------------|------------------------|------------------------|
| 20 | $y = 0.0819x + 3.3162$ | $y = 0.0722x + 3.6451$ | $y = 0.0642x + 3.8559$ |
| 30 | $y = 0.0961x + 3.4225$ | $y = 0.0668x + 3.8901$ | $y = 0.087x + 4.0255$ |
| 40 | $y = 0.1552x + 3.4563$ | $y = 0.0994x + 4.0251$ | $y = 0.139x + 4.2301$ |

The value of the angular coefficient naturally grows with an increase in temperature.

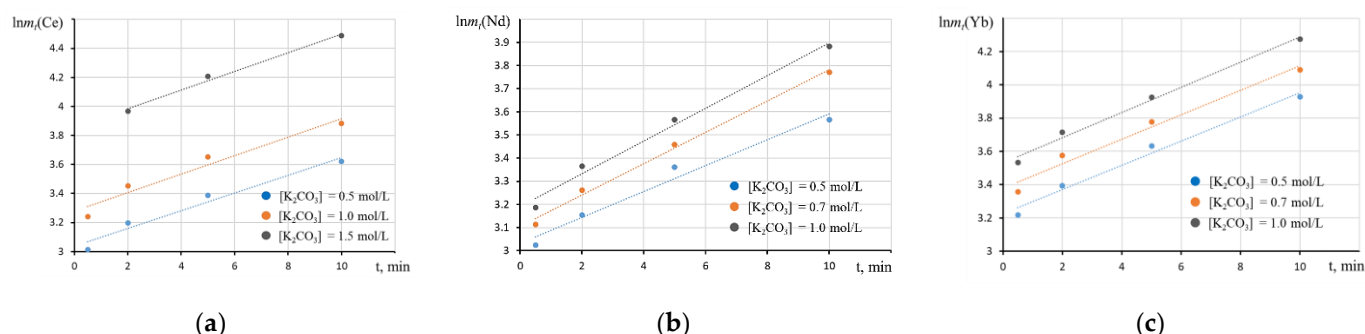


Figure 6. Time-dependent logarithm of weight obtained by dissolving lanthanide carbonate at a temperature of 20 °C: (a) for Ce; (b) for Nd; (c) for Yb.

Table 7 shows the linear relationships that are described by empirical equations.

Table 7. Empirical dependence of the degree of recovery into the solution on the concentration of potassium carbonate.

| [K ₂ CO ₃], mol/L | Dependency Equation (Nd) | Dependency Equation (Yb) |
|--|--------------------------|--------------------------|
| 0.5 | y = 0.0559x + 3.0316 | y = 0.0729x + 3.2243 |
| 0.7 | y = 0.0678x + 3.1042 | y = 0.0735x + 3.3784 |
| 1 | y = 0.0708x + 3.1905 | y = 0.0754x + 3.5312 |
| [K ₂ CO ₃], mol/L | Dependency Equation (Ce) | - |
| 0.5 | y = 0.0611x + 3.037 | - |
| 1 | y = 0.0639x + 3.278 | - |
| 1.5 | y = 0.0642x + 3.856 | - |

The values of angular coefficients, obtained for different concentrations, differ slightly from each other, which can be explained by some error in the performance of experimental studies. The value of the angular coefficient of semilog dependencies is the mass transfer coefficient (reaction rate constant) and the average values, which are 0.0631 for cerium, 0.0648 for neodymium, and 0.0739 for ytterbium.

If the process conditions are constant, then the initial concentration of the reagent, its amount, size, and shape, the flow rate of the mobile phase, and the apparent activation energy of the process can be calculated from the temperature dependence of the conversion rate of the substance, at an arbitrarily selected (equal for all temperatures) conversion degree, in accordance with the following equation:

$$\frac{(d\alpha/dt)_{T_1}}{(d\alpha/dt)_{T_2}} = \frac{k_{T_1}(m_0 - \alpha v m_0)^n}{k_{T_2}(m_0 - \alpha v m_0)^n} = \frac{k_{T_1}}{k_{T_2}}$$

Taking into account the Arrhenius equation, as follows:

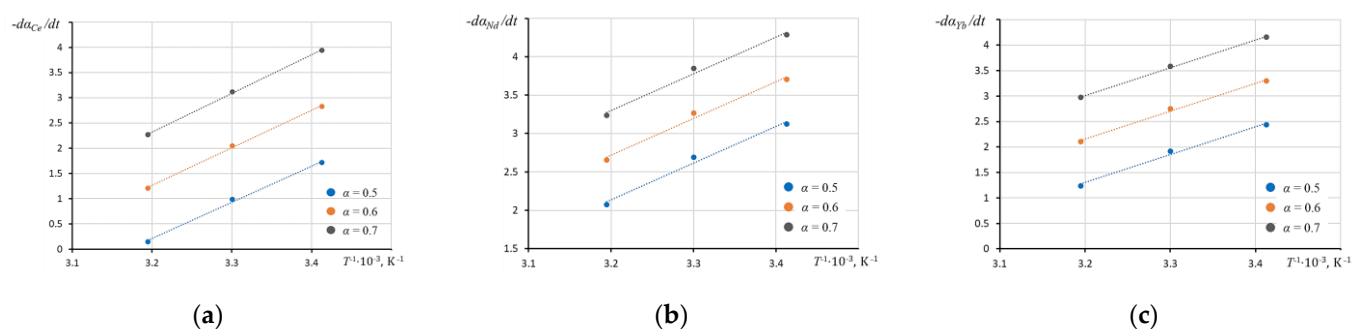
$$k = Ae^{-\frac{E_a}{RT}}$$

$$\ln \left[\frac{(d\alpha/dt)_{T_1}}{(d\alpha/dt)_{T_2}} \right] = \ln \left(\frac{k_{T_1}}{k_{T_2}} \right) = -\frac{E}{R} \left(\frac{1}{T_1} - \frac{1}{T_2} \right)$$

or

$$\ln \left(\frac{d\alpha}{dt} \right) = -\frac{E_a}{R} \left(\frac{1}{T} \right)$$

The semilog relationship between the leaching rate and the inverse temperature is shown in Figure 7.

**Figure 7.** Leaching rate versus return temperature: (a) for Ce; (b) for Nd; (c) for Yb.

Linear dependencies are approximated by the equations shown in Table 8, with an approximation validity value of at least 98%.

Table 8. Linear approximation of leaching data.

| T, °C | Nd | Yb | Ce |
|-------|------------------------|------------------------|------------------------|
| 20 | $y = 4.7987x - 13.22$ | $y = 5.4689x - 16.199$ | $y = 7.1671x - 22.721$ |
| 30 | $y = 4.7989x - 12.639$ | $y = 5.4584x - 15.311$ | $y = 7.4179x - 22.47$ |
| 40 | $y = 4.799x - 12.059$ | $y = 5.448x - 14.422$ | $y = 7.6687x - 22.218$ |

The angular coefficient of dependencies is proportional to the activation energy. The calculated value of the activation energy is also presented in Table 9. The apparent activation energy of lanthanides ranges from 30 to 61 kJ/mol, which is characteristic of diffusion or transient modes.

Table 9. Kinetic parameters of carbonate dissolution of lanthanide precipitates.

| Element | Activation Energy, kJ/mol | Arrhenius Constant, min ^{−1} | Apparent Order of Reaction n |
|---------|---------------------------|---------------------------------------|------------------------------|
| Ce | 61.6 | 1.29×10^{10} | 1.00 |
| Nd | 39.9 | 1.85×10^{10} | 1.00 |
| Yb | 45.4 | 1.47×10^{10} | 1.00 |

For heterogeneous solid–liquid systems, where a dissolution reaction of a slightly soluble compound occurs, a first-order reaction is characteristic, which was confirmed experimentally. The presented kinetic data describe the complex process of diffusion of the complexing agent–carbonate ion to the surface of the lanthanide precipitate, dissociation and formation of the complex compound; in this regard, the system under consideration cannot be called ideal. An important consideration is the size of the precipitate and the degree of amorphism.

5. Conclusions

Analysis of the kinetic parameters of the dissolution of lanthanide precipitates and the formation of carbonate complexes allows us to conclude on the complexity of the process. Various factors must be taken into account, as follows: the temperature of the system, the concentration of carbonate ion—which acts as a complexing agent—the influence of mixing intensity, and the nature of the reacting substances. Empirical equations were obtained, describing the dependence of dissolution of lanthanide carbonate on these factors.

The data obtained indicate the predominantly diffusion nature of the process of dissolving lanthanide precipitates, as indicated by the dependence of the degree of recovery on the stirring rate, the first reaction order, and the relatively low activation energy—dissolution of cerium carbonate 61.6 kJ/mol, ytterbium carbonate 45.4 kJ/mol, and neodymium carbonate 39.9 kJ/mol. The Arrhenius constant was used for dissolving cerium carbonate $1.29 \times 10^{10} \text{ min}^{-1}$, ytterbium carbonate $1.47 \times 10^{10} \text{ min}^{-1}$, and neodymium carbonate $1.85 \times 10^{10} \text{ min}^{-1}$.

The results of the study can be used in modeling the process of carbonation of technogenic raw materials and extraction of rare earth metals. Maintaining the process at optimal parameters will allow one to obtain the greatest degree of extraction, to reduce energy and capital costs for implementation, to increase profitability, and to increase the depth of processing of mineral raw materials.

Author Contributions: Conceptualization, T.L. and R.K.; methodology, R.K.; validation, S.G., R.K. and I.Z.; data curation, I.Z.; writing—original draft preparation, R.K.; writing—review and editing, S.G.; supervision, T.L.; project administration, T.L. All authors have read and agreed to the published version of the manuscript.

Funding: The study was carried out at the expense of a subsidy for the implementation of the state task in the field of scientific activity for 2021 №FSRW-2020-0014.

Institutional Review Board Statement: Not applicable.

Informed Consent Statement: Not applicable.

Data Availability Statement: Data are presented in this article.

Conflicts of Interest: The authors declare no conflict of interest.

References

1. Binnemans, K.; Jones, P.T.; Blanpain, B.; Gerven, T.V.; Pontikes, Y. Towards zero-waste valorization of rare-earth-containing industrial process residues. *J. Clean. Prod.* **2015**, *99*, 17–38. [\[CrossRef\]](#)
2. Bykhovsky, L.Z.; Arkhangelskaya, V.V.; Tigunov, L.P.; Anufrieva, S.I. Prospects for the development of the mineral resource base and the development of production. *VIMS Miner. Raw Mater.* **2007**, *22*, 45.
3. Pyagai, I.N.; Kozhevnikov, V.L.; Pasechnik, L.A.; Skachkov, V.M. Processing of slime of alumina production with extraction of scandium concentrate. *J. Min. Inst.* **2016**, *218*, 225–232.
4. Chaschina, E.S.; Bagnavets, N.L. Use of phosphoric acid purified by extraction method for production of phosphorus fertilizers. *News RSAU-MTAA* **2010**, *5*, 151–155.
5. Kochetkov, S.P.; Smirnov, N.N.; Ilyin, A. Concentration and Purification of Extraction Phosphoric Acid. *Solvent Extr. Res. Dev. Jpn.* **2007**, *304*, 23–35.
6. Rutherford, P.M.; Dudas, M.J.; Samek, R.A. Environmental impacts of phosphogypsum. *Sci. Total Environ.* **1994**, *149*, 1–38. [\[CrossRef\]](#)
7. Evan, K. The history, challenges and new developments in the management and use of bauxite residue. *J. Sustain. Met.* **2016**, *2*, 316–331. [\[CrossRef\]](#)
8. Ritters, S.K. Making the most of red mud. *C EN* **2014**, *92*, 33.
9. Utkov, V.A.; Sizyakov, V.M. Modern issues of metallurgical processing of red sludge. *J. Min. Inst.* **2013**, *202*, 39–43.
10. Trushko, V.L.; Utkov, V.A.; Bazhin, V.Y. Relevance and ways of full processing of red mud from alumina production. *J. Min. Inst.* **2017**, *227*, 547–553.
11. Besedin, A.A.; Utkov, V.A.; Brichkin, V.N.; Sizyakov, V.M. Agglomeration sintering of red sludge. *Obogashchenie Rud* **2014**, *2*, 28–31.
12. Sabirzyanov, N.A.; Yatsenko, S.P. *Hydrochemical Methods of Complex Processing of Bauxite*; Ural RAS: Ekaterinburg, Russia, 2006.
13. Tsakiridis, P.E.; Agatzini-Leonardou, S.; Oustadakis, P. Red mud addition in the raw meal for the production of Portland cement clinker. *J. Hazard. Mater.* **2004**, *116*, 103–110. [\[CrossRef\]](#)
14. Cakici, A.I.; Yanik, J.; Karayildirim, T.; Anil, H. Utilization of red mud as catalyst in conversion of waste oil and waste plastics to fuel. *J. Mater. Cycles Waste Manag.* **2004**, *6*, 20–26.
15. Stepanov, S.I.; Aung, M.M.; Aung, H.J.; Boyarintsev, A.V. Chemical aspects of carbonate leaching of scandium from red sludges. *Bull. VGUIT* **2018**, *4*, 349–355.
16. Dubovikov, O.A.; Brichkin, V.N.; Besedin, A.A. Dehydration of red sludge and the main directions of its processing. *Obogashchenie Rud* **2014**, *1*, 44–49.
17. Zubkova, O.S.; Alekseev, A.I.; Zalilova, M.M. Research of combined use of carbon and aluminum compounds for wastewater treatment. *Izv. Vyss. Uchebnykh Zaved. Seriya Khim. Khim. Tekhnol.* **2020**, *63*, 86–91. [\[CrossRef\]](#)
18. Borra, C.R.; Mermans, J.; Blanpain, B.; Pontikes, Y.; Binnemans, K.; Gerven, T.V. Selective leaching of rare earths from bauxite residue after sulphation roasting. In Proceedings of the Bauxite Residue Valorization and Best Practices Conference, Leuven, Belgium, 5–7 October 2015; pp. 301–308.
19. Tsai, H.S.; Tsai, T.H. Extraction Equilibrium of Indium(III) from Nitric Acid Solutions by Di(2-ethylhexyl)phosphoric Acid Dissolved in Kerosene. *Molecules* **2012**, *17*, 408–419. [\[CrossRef\]](#)
20. Wu, S.; Wang, L.; Zhang, P.; El-Shall, H.; Moudgil, B.; Huang, X.; Zhao, L.; Zhang, L.; Feng, Z. Simultaneous recovery of rare earths and uranium from wet process phosphoric acid using solvent extraction with D2EHPA. *Hydrometallurgy* **2018**, *175*, 109–116. [\[CrossRef\]](#)
21. Batchu, N.K.; Binnemans, K. Effect of the diluent on the solvent extraction of neodymium(III) by bis(2-ethylhexyl)phosphoric acid (D2EHPA). *Hydrometallurgy* **2018**, *177*, 146–151. [\[CrossRef\]](#)
22. Alberts, E. *Stripping Rare Earth Elements and Iron from D2EHPA during Zinc Solvent Extraction*; Stellenbosch University: Stellenbosch, South Africa, 2011; p. 121.
23. Papkova, M.V.; Mikhailichenko, A.I.; Konkova, T.V. Sorption extraction of rare-earth elements from phosphoric acid solutions. *Sorption Chromatogr. Process.* **2016**, *16*, 163–172.
24. Martín, D.M.; Jalaff, L.D.; García, M.A.; Faccini, M. Selective recovery of europium and yttrium ions with cyanex 272-polyacrylonitrile nanofibers. *Nanomaterials* **2019**, *9*, 1648. [\[CrossRef\]](#)
25. Weilert, A.V.; Pyagai, I.N.; Kozhevnikov, V.L.; Pasechnik, L.A.; Yatsenko, S.P. Autoclave-hydrometallurgical processing of red clay sludge. *Non-Ferr. Met.* **2014**, *3*, 31–35.
26. Medvedev, A.S.; Khayrullina, R.T.; Kirov, S.S.; Suss, A.G. Technical scandium oxide obtaining from red mud of Urals Aluminium Smelter. *Non-Ferr. Met.* **2015**, *12*, 47–52. [\[CrossRef\]](#)
27. Medvedev, A.S.; Kirov, S.S.; Khayrullina, R.T.; Suss, A.G. Carbonization leaching of scandium from red mud with preliminary pulp gassing by carbonic acid. *Non-Ferr. Met.* **2016**, *6*, 67–73. [\[CrossRef\]](#)

-
28. Cheremisina, O.V.; Sergeev, V.V.; Fedorov, A.T.; Alferova, D.A. Separation of rare-earth metals and titanium in complex apatite concentrate processing. *Obogashchenie Rud* **2020**, *5*, 30–34. [[CrossRef](#)]
 29. Cheremisina, O.V.; Cheremisina, E.; Ponomareva, M.A.; Fedorov, A.T. Sorption of rare earth coordination compounds. *J. Min. Inst.* **2020**, *244*, 474–481. [[CrossRef](#)]
 30. Lebedev, I.A.; Kulyako, Y.M. Thermodynamic stability constants of phosphate complexes. *WNH* **1978**, *23*, 3215–3227.
 31. Spahiu, K.; Bruno, J. A Selected Thermodynamic Database for REE to be Used in HLNW Performance Assessment Exercises. *MBT Technol. Ambient.* **1995**, *28*, 2–22.
 32. Ravikumar, B.; Ramaswamy, S.; Pandiarajan, S. FTIR and laser RAMAN spectral analysis of crystalline DL-valinium dihydrogen phosphate. *Int. J. Eng. Sci. Technol.* **2012**, *4*, 1658–1666.
 33. Kashurin, R.R.; Gerashev, S.A.; Litvinova, T.E.; Zhadovskiy, I.T. Prospective recovery of rare earth elements from waste. *J. Phys. Conf. Ser.* **2020**, *1679*, 052070. [[CrossRef](#)]
 34. Ermakova, N.V.; Burmaa, D.; Ivanov, V.M.; Figurovskaya, V.N. Definition of lanthanum (III), terbium (III) and erbium (III) in alkali metal halides and sulphates doped with rare earth elements. *Mosc. Univ. Chem. Bull.* **2000**, *41*, 305–308.
 35. Gupta, C.K. *Chemical Metallurgy: Principles and Practice*; Wiley-VCH Verlag GmbH & Co.: Hoboken, NJ, USA, 2003; pp. 322–327.
 36. Liu, Z.; Dreybrodt, W. Dissolution kinetics of calcium carbonate minerals in H₂O-CO₂ solutions in turbulent flow: The role of the diffusion boundary layer and the slow reaction $\text{H}_2\text{O} + \text{CO}_2 = \text{H}^+ + \text{HCO}_3^-$. *Geochim. Cosmochim. Acta* **1997**, *61*, 2879–2889. [[CrossRef](#)]
 37. Wang, Y.; Abrahamsson, B.; Lindfors, L.; Brasseur, J. Analysis of Diffusion-Controlled Dissolution from Polydisperse Collections of Drug Particles with an Assessed Mathematical Model. *J. Pharm. Sci.* **2015**, *104*, 2998–3017. [[CrossRef](#)] [[PubMed](#)]